Available online at www.sciencedirect.com
ScienceDirect
Comparative Biochemistry and Physiology, Part C 147 (2008) 424–433
CBP
www.elsevier.com/locate/cbpc

Self-proteolysis regulation in the *Bothrops jararaca* venom: The metallopeptidases and their intrinsic peptidic inhibitor ☆

Rafael Marques-Porto [a], Ivo Lebrun [b], Daniel C. Pimenta [b,*]

[a] *CAT/CEPID, Instituto Butantan, Av Vital Brasil, 1500, São Paulo – SP, 05503-900, Brazil*
[b] *Laboratório de Bioquímica e Biofísica, Instituto Butantan, Av Vital Brasil, 1500, São Paulo – SP, 05503-900, Brazil*

Received 29 November 2007; received in revised form 22 January 2008; accepted 22 January 2008
Available online 5 February 2008

Abstract

Snake venom proteome variation is a well-documented phenomenon, whereas peptidome variation is still relatively unknown. We used a biological approach to explore the inhibitory activities present in the whole venom of *Bothrops jararaca* that prevents the venom self-proteolysis and/or digestion of the glandular tissue. Although snake venom metallopeptidases have long been known from the biochemical up to the clinical point of view, the mechanisms by which these enzymes are regulated in the reptile's venom gland remain fairly unknown. We have successfully demonstrated that there are three synergistic weak inhibitory mechanisms that are present in the crude venom that are able to abolish the metallopeptidase activity in situ, namely: (i) citrate calcium chelation; (ii) acidic pH and; (iii) enzymatic competitive inhibition by the tripeptide Pyroglutamyl-lysyl-tryptophan. Taken together, these three factors become a strong set-up that inhibits the crude venom metallopeptidase activity as well as a purified metallopeptidase from this same venom. However, this inhibition can be totally reverted by dilution into an optimal pH solution, such as the blood.

Keywords: Metallopeptidase; Mass spectrometry; *Bothrops jararaca*; Snake venom; Inhibitors; Peptides

1. Introduction

Snake venoms are recognized for their biochemical complexity. Any given viperid venom may contain several thousand proteins (Fox et al., 2002), most of which are hydrolases, including metallopeptidases, serine-peptidases and phospholipases A2. Also present in large amounts are peptides, mostly bradykinin potentiating peptides (BPPs) (Ianzer et al., 2004). Understanding the mechanisms in which these components are involved within the crude venom and in the process of envenomation is therefore a challenge. Furthermore, the resultant variety of targets with which venom toxins specifically interact make them potential candidates for the design of drugs and biological tools.

Snake venom metallopeptidases (SVMPs), which represent up to 53% of all peptidase transcripts in viperid venoms, as in *Bothrops jararaca* (Cidade et al., 2006), play an important role in envenomation by these snakes, causing severe hemorrhage, tissue necrosis and inhibition of platelet aggregation in the victim's organism (Jia et al., 1997). Although SVMPs are highly active against the victim's tissues, they do not affect the venom's own components or the venom gland tissues. Few studies exist on the subject, like Sousa et al.'s (2001) assessing the proteolytic action of *Bothrops* venom upon its own components. Therefore, a mechanism of inhibition of the SVMPs that would become inactive as the venom is delivered to the victim must exist in the venom. Calcium ions stabilize

Abbreviations: ACN, acetonitrile; ADAM, a disintegrin and metallopeptidase; BPP(s), Bradykinin potentiating peptide(s); CID, collision induced dissociation; ESI, electrospray ionization; FRET, Fluorescence resonance energy transfer; MMP, matrix metallopeptidase; MS, mass spectrometry; MS/MS, tandem mass spectrometry; Q-TOF, orthogonal quadrupole-time-of-flight (mass spectrometry); RP-HPLC, reversed-phase high performance liquid chromatography; SVMP, snake venom metallopeptidase; TFA, trifluoroacetic acid.

☆ This work was developed by R Marques-Porto and DC Pimenta when working at the Center for Applied Toxinology – CAT/CEPID, Instituto Butantan, Av Vital Brasil, 1500, São Paulo, SP – 05503-900, Brazil – phone/fax (+55 11) 3726-1024.

* Corresponding author. Avenida Vital Brazil, 1500, São Paulo – SP, 05503-900, Brazil. Tel.: +55 11 3726 7222x2101; fax: +55 11 3726 7222x2018.
E-mail address: dcpimenta@butantan.gov.br (D.C. Pimenta).

1532-0456/$ - see front matter © 2008 Elsevier Inc. All rights reserved.
doi:10.1016/j.cbpc.2008.01.011

SVMPs (Moura-da-Silva et al., 2003) and activate matrix metallopeptidases (MMPs) in general (Gossas and Danielson, 2006) and it has been shown that citrate is present in viperid venom at a concentration between 58 and 125 mM, (Odell et al., 1998) which is enough to chelate all of the venom's free calcium. Moreover, this high citrate concentration inhibits the venom proteases activity up to 80% (for *Bothrops picadoi*, at 27 mM citrate concentration) and may serve as an anticoagulant in the prey (Odell et al., 1998). Furthermore, Pyroglutamyl-tripeptide inhibitors have also been described in viperid venoms as able to inhibit the metallopeptidase activities (Huang et al., 1998).

All metallopeptidases in viperid venoms characterized to date are of the reprolysin family, of the metzincins clan. Fox and Serrano (2005) have recently reviewed the subject and present interesting outlines on the structural classification of these enzymes. Briefly, the SVMP all present the extended Zn coordination site HEXXHXXGXXH and the structure of the active site is highly conserved among them. Structurally, they are closely related to the ADAMs (a disintegrin and metallopeptidase), mammalian proteins involved in cell activation and communication and to MMPs. They are found in different processing states of similar zymogen multidomain precursors: P-I SVMPs contain only the catalytic domain, while in P-III SVMPs, disintegrin-like/cysteine-rich domains are added to the catalytic domain. The catalytic domain shares great functional and structural similarity with the metallopeptidase domain of MMPs (Blundell, 1994), conserving all the zinc-binding residues and structural constraints involved in catalysis.

Understanding the mechanisms in which SVMPs are involved, and more specifically how they are controlled and inhibited inside the venom gland, might provide tools for the development of drugs designed to control diseases in which metallopeptidases structurally similar to SVMPs play a part. In this work, we have assessed the *B. jararaca* venom's metallopeptidase activity over a synthetic peptidic substrate and identified an intrinsic tripeptide inhibitor (<EKW, being <E pyroglutamic acid) of this activity, which has also been found in *Trimeresurus mucrosquamatus*) (Huang et al., 1998). Furthermore, we have compared the whole venom metallopeptidase activity to isolated Bothropasin, a typical P-III SVMP from *B. jararaca* (Mandelbaum et al., 1982; Assakura et al., 2003) and were able to determine a direct correlation between these enzymatic activities.

2. Materials and methods

2.1. Reagents

Sephadex G-25 (Pharmacia, Upsalla, Sweden), α-cyano-4-hydroxycinnamic acid, peptide molecular mass standards and the chemicals and salts employed were obtained from Sigma Co (St Louis, MO, USA). Bothropasin was a kind gift of Dr Ana Moura-da-Silva (Instituto Butantan, São Paulo, Brasil).

2.2. Venom samples

B. jararaca venom was supplied by the venom section of Instituto Butantan in lyophilized form. This venom pool is constituted of venom extracted from circa 1000 specimens (male and female, adult and young) captured/originated from all the animal's habitats. Briefly, venom extracted from several snakes was centrifuged at 1509 g for 30 min at 4 °C. The supernatant was frozen at −20 °C and lyophilized. The material was stored at −20 °C. Alternatively, the fresh venom, extracted from three adult specimens (two females and one male), was separated in 100 μL aliquots and frozen at −20 °C until use.

2.3. Purification procedures

2.3.1. Size exclusion chromatography

A 700 mg lyophilized crude venom aliquot was resuspended in 1.5 mL 50 mM ammonium acetate buffer, pH 4.0, and loaded onto a Sephadex G-25 column (101 × 1.2 cm, 120 mL). The material was eluted using the same buffer at a constant flow rate of 1.2 mL min^{-1} and monitored by its absorbance at 214 nm and 280 nm. One mL fractions were collected and pooled according to Fig. 1.

2.3.2. Reversed-phase chromatography

Reversed-phase binary HPLC system (10AVp, Shimadzu Co., Japan) was used for sample separation. The lyophilized size exclusion-fractionated sample was loaded into a Shimadzu C18 column (Shin Pack 5 μ, 4.6 × 250 mm) in a two-solvent system: (A) trifluoroacetic acid (TFA)/H_2O (1:1000) and (B) TFA/Acetonitrile (ACN)/H_2O (1:900:100). The column was eluted at a flow rate of 1 mL min^{-1} with a 10 to 80% gradient of solvent B over 60 min. The HPLC column eluates were monitored by their absorbance at 214 nm (SPD-10AV) and/or by their fluorescence emission at 420 nm after excitation at 320 nm (RF-10Ax) for the FRET peptides. For peptides purification, further chromatographic steps were necessary, using the same column with optimized gradients.

2.4. Mass spectrometry

Molecular mass analyses of the fractions and purified peptides were performed on a Q-TOF Ultima API (Micromass, Manchester, UK), under positive ionization mode and/or by MALDI/TOF mass spectrometry on an Ettan MALDI-TOF/Pro system (Amersham Biosciences, Sweden), using α-cyano-4-hydroxycinnamic acid as matrix.

2.4.1. de novo peptide sequencing

Mass spectrometric 'de novo' peptide sequencing was carried out in positive ionization mode on a Q-TOF Ultima API fitted with an electrospray ion source (Micromass, Manchester, UK). The samples were dissolved into a mobile phase of 50:50 aqueous formic acid 0.1%/ acetonitrile and directly injected (10 μL) using a Rheodyne 7010 sample loop coupled to a LC-10A VP Shimadzu pump at 20 μL/min, constant flow rate. The instrument control and data acquisition were conducted by MassLynx 4.0 data system (Micromass, Manchester, UK) and experiments were performed by scanning from a mass-to-charge ratio (m/z) of 50 to 1800 using a scan time of 2 s applied during the whole infusion. The mass spectra corresponding to each

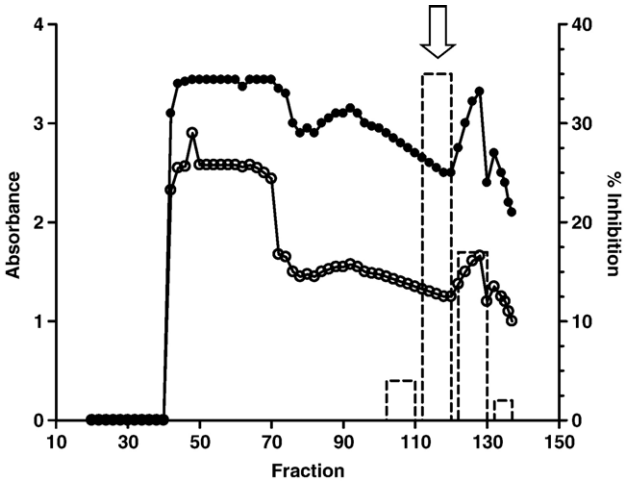

Fig. 1. Size exclusion chromatography of the whole *Bothrops jararaca* venom. Separation was performed on a Sephadex G-25 column, eluted with 50 mM ammonium acetate, pH 4 at 1.2 mL min^{-1} flow rate. The 1 mL fractions were pooled every 7 mL. The profile was monitored at 214 nm (○) and 280 nm (●). Dashed line: Inhibition of the venom metallopeptidase activity. (right axis) Percentage of the residual hydrolytic activity over Abz-GGFLTSE-Q-EDDnp (10 μM) observed after the addition of 10 μL of the pooled fraction on the hydrolysis of the FRET substrate by 10 μg mL^{-1} crude *B. jararaca* venom in 50 mM Tris–HCl, pH 7.4 at 37 °C. The white arrow indicates the selected pool (113–119) submitted to further fractionation.

signal from the total ion current (TIC) chromatogram were averaged, allowing an accurate molecular mass determination. External calibration of the mass scale was performed with NaI. For the MS/MS analysis, collision energy ranged from 18 to 45 eV and the precursor ions were selected under a $1-m/z$ window. Amino acid analyses were performed to quantify the peptides purified throughout this work.

2.5. Synthetic peptide

The FRET substrate Abz-GGFLTSE-Q-EDDnp was synthesized and kindly supplied by Dr Maria Aparecida Juliano from Departamento de Biofísica, Escola Paulista de Medicina – UNIFESP. The FRET peptide contains the *o*-aminobenzoic acid (Abz) at the N-terminus of the peptide, as the fluorescent donor, and *N*-[2,4-dinitrophenyl]-ethylenediamine (EDDnp, the quencher) attached to a C-terminal glutamine, a necessary result of the solid-phase peptide synthesis strategy employed.

2.6. Enzymatic profiling

2.6.1. Enzymatic assays

Hydrolysis of the FRET substrate in 50 mM Tris–HCl, pH 7.4 at 37 °C was monitored by measuring the fluorescence at λ_{em}=420 nm and λ_{ex}=320 nm in a Hitachi F-2000 spectrofluorometer. The 1 cm path-length cuvette containing 1 mL of the substrate solution was placed in a thermostatically controlled cell compartment for 5 min before the enzyme solution was added and the increase in fluorescence with time was continuously recorded for up to 10 min. The slope was converted into moles of

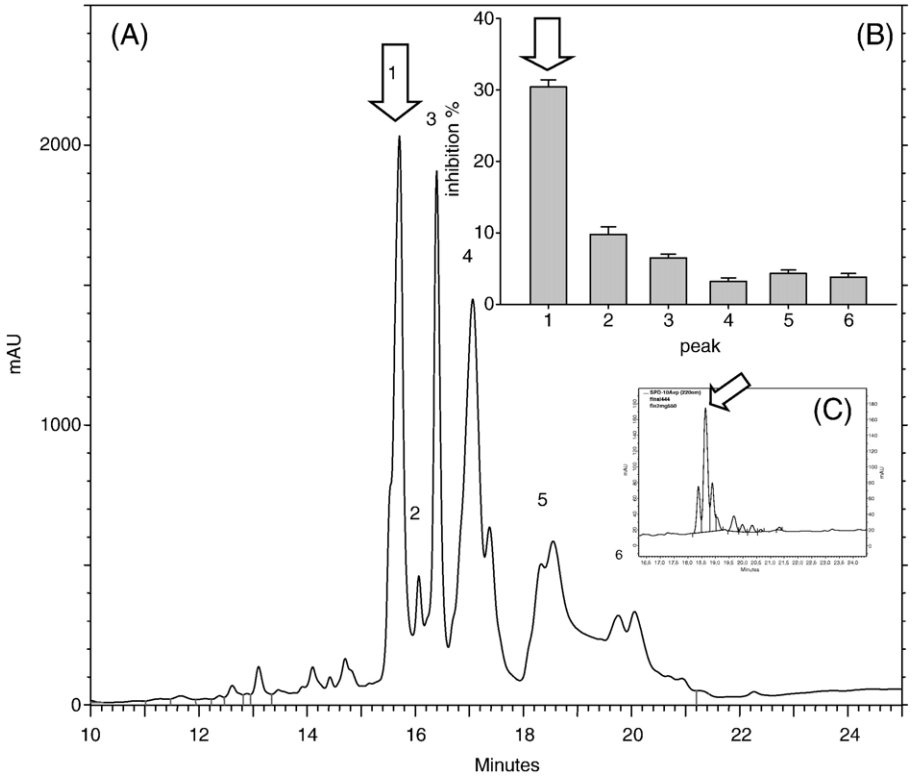

Fig. 2. (A) RP-HPLC profile of the size exclusion pool 113–119 monitored at λ=214 nm. (B) Inhibition of the venom metallopeptidase activity. Percentage of the residual hydrolytic activity over Abz-GGFLTSE-Q-EDDnp (10 μM) observed after the addition of 10 μL of the pooled fraction on the hydrolysis of the FRET substrate by 10 μg mL^{-1} crude *B. jararaca* venom in 50 mM Tris–HCl, pH 7.4 at 37 °C. *The white arrow indicates the selected peak 1 submitted to further fractionation. (C) RP-HPLC re-chromatographic separation of peak 1, under the same conditions. The white arrow indicates the selected peak submitted to further fractionation and MS and/or MS/MS characterization (Fig. 7).

hydrolyzed substrate per minute based on the fluorescence curves of standard peptide solutions before and after total enzymatic hydrolysis. The concentration of the peptide solutions was determined by colorimetric determination of the 2,4-dinitrophenyl group ($\varepsilon_{365\ nm}$=17,300 M^{-1} cm^{-1}). The enzyme (or venom) concentration for initial rate determination was chosen at a level

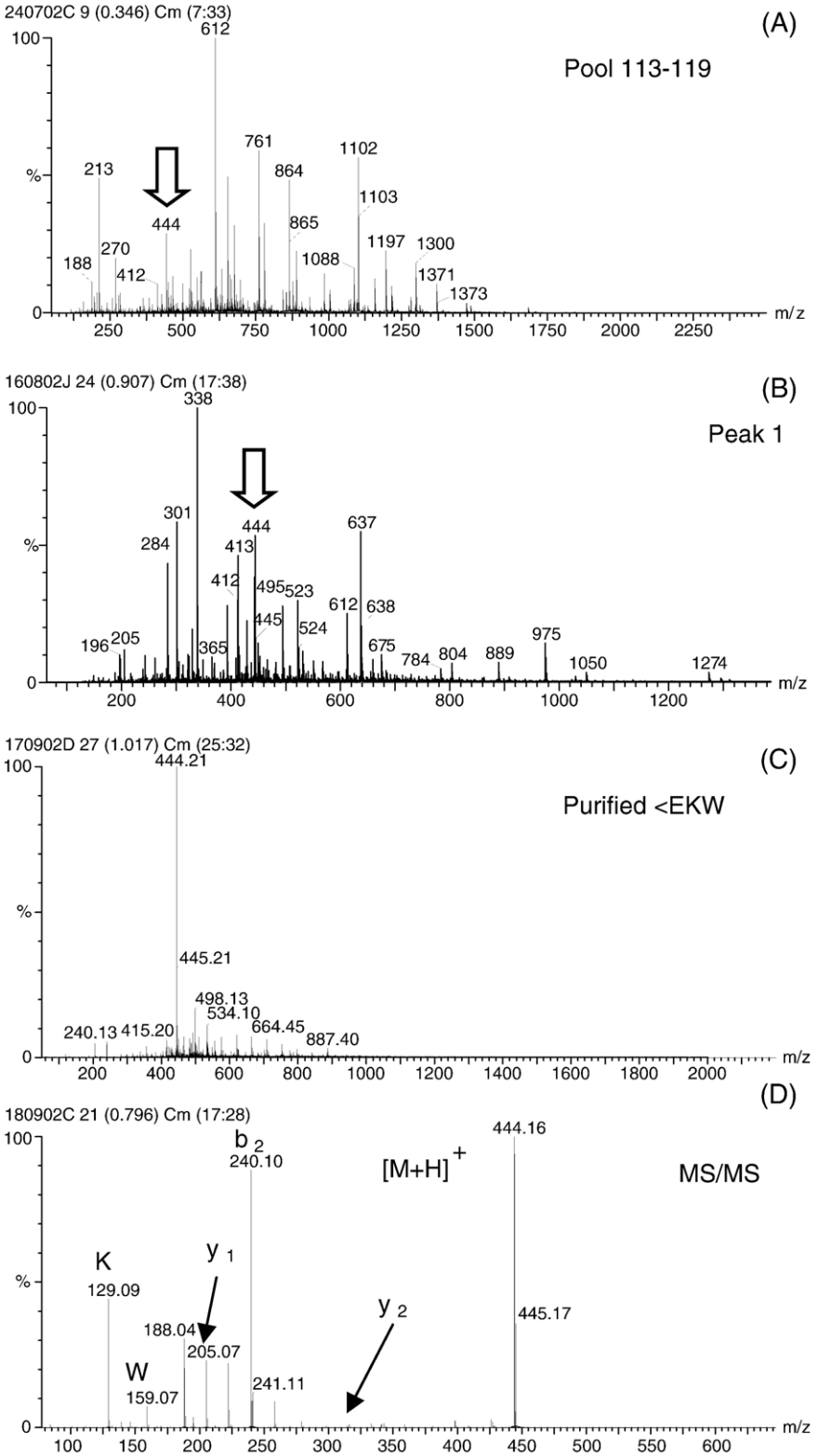

Fig. 3. Representative mass spectrometry data. Positive ESI-Q-TOF profiles of: (A) pooled fractions 113–119 (Fig. 1); (B) RP-HPLC peak 1, pre-purified fraction 113–119 (Fig. 2A); (C) RP-HPLC peak 2 of purified <EKW (Fig. 2C) and (D) MS/MS profile of <EKW, used for de novo sequencing of the peptide, showing some representative daughter ions. White arrows (panels A and B) point out to the *m/z* corresponding to <EKW.

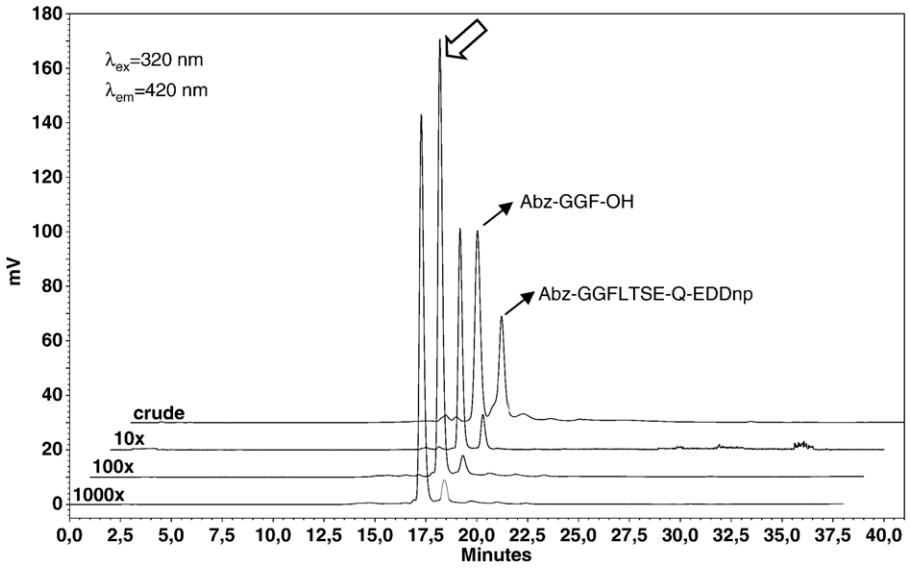

Fig. 4. Enzymatic activation through dilution. Representative pH profiles of incubated Abz-GGFLTSE-Q-EDDnp, in 50 mM Tris–HCl, containing 1 mM $CaCl_2$, pH 7.4 at 37 °C, with crude *B. jararaca* venom and the serially diluted aliquots (10, 100 and 1000 times) monitored by fluorescence at the indicated wavelengths. The white arrow indicates the peak of activity at 100-fold venom dilution.

intended to hydrolyze less than 5% of the substrate present, when $[S] > K_M$.

2.6.2. pH profile and salt effect

Pseudo first-order conditions were employed for the initial velocities determinations for both the pH profiling and the salt effect assessment. The data were then fitted into non-linear least-square equations for the estimation of the rate. For pH profiling the following buffered solutions were employed, with 0.25 pH unit pace and duplicate assays on overlapping pH buffers: 50 mM sodium acetate (pH 3.0–5.5), 50 mM sodium phosphate (pH 5.5–8.0), 50 mM Tris–HCl (pH 8.0–9.0), 50 mM glycine (pH 9.0–9.5). For salt effect and calcium modulation assays, 50 mM Tris–HCl, pH 7.4 was the buffer of choice containing the different salt concentrations assayed.

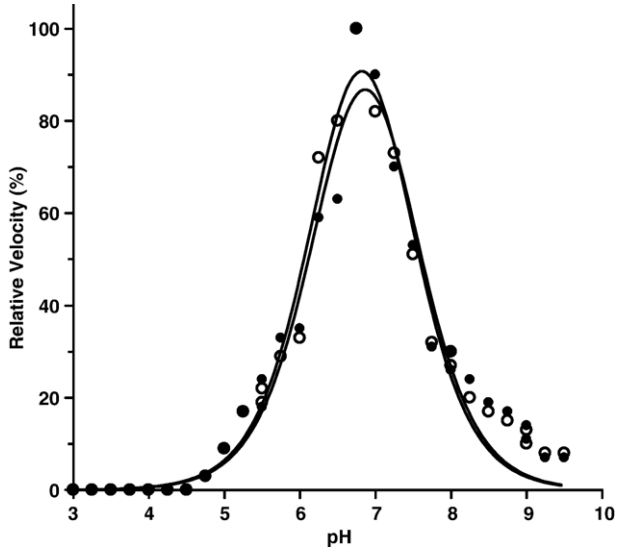

Fig. 5. Relative velocity pH dependence of 10 μg mL^{-1} crude venom (○) and 0.1 mg mL^{-1} Bothropasin (●) proteolytic activity over Abz-GGFLTSE-Q-EDDnp (10 μM). Calculated pK_a values: 6.35±0.10 and 7.28±0.10 (venom) and 6.35±0.12 and 7.37±0.11 (Bothropasin). Proportional rate of hydrolysis is shown as a function of the highest rate, for each activity.

2.6.3. RP-HPLC enzymatic dilution assay

Hydrolysis of the FRET substrate by either the crude venom or by venom aliquots diluted into 50 mM Tris–HCl, pH 7.4 at 37 °C was monitored by RP-HPLC as described above. Five μL buffered substrate solution (5 μM final concentration) was added to a 20 μL fresh venom sample (crude or serially diluted) and incubated for 10 min at 37 °C. The reaction was stopped by the addition of 75 μL 1% TFA followed by freezing. The fluorescent column eluates were collected and subjected to mass spectrometry in order to confirm the cleavage site.

2.7. Statistical analyses

When data fitting was performed, results are presented as the calculated value±SD. Otherwise; data correspond to the mean of three individual experiments.

3. Results

3.1. Chromatographic separation

3.1.1. Size exclusion chromatography

Fig. 1 presents the Sephadex G-25 chromatographic profile of 700 mg pooled *B. jararaca* venom, together with the inhibition profiling of the pooled fractions. The separation was monitored at 214 and 280 nm and the eluates were fractionated into 1 mL samples, as described in the Materials and methods section. Then, the fractions were pooled every 7 mL to in order to enrich its contents and these pools were assayed for venom metallopeptidase activity inhibition. Among the active pools (represented by their proportional inhibition rate in dashed bars

in Fig. 1), only pool 113–119 was elected for further biochemical characterization.

3.1.2. Reversed-phase HPLC

Fraction 113–119 originated from the size exclusion chromatography was further fractionated by RP-HPLC, as presented in Fig. 2A. The peaks were monitored and separated by their absorbance at 214 nm, and were tested for venom metallopeptidase activity inhibition (Fig. 2B). Peak 1 (white arrow) was submitted to mass spectrometric analysis (Fig. 3B) and a subsequent RP-HPLC re-chromatography, for characterization and identification of the peptide molecule responsible for the enzymatic inhibition (Figs. 2C, 3C and D).

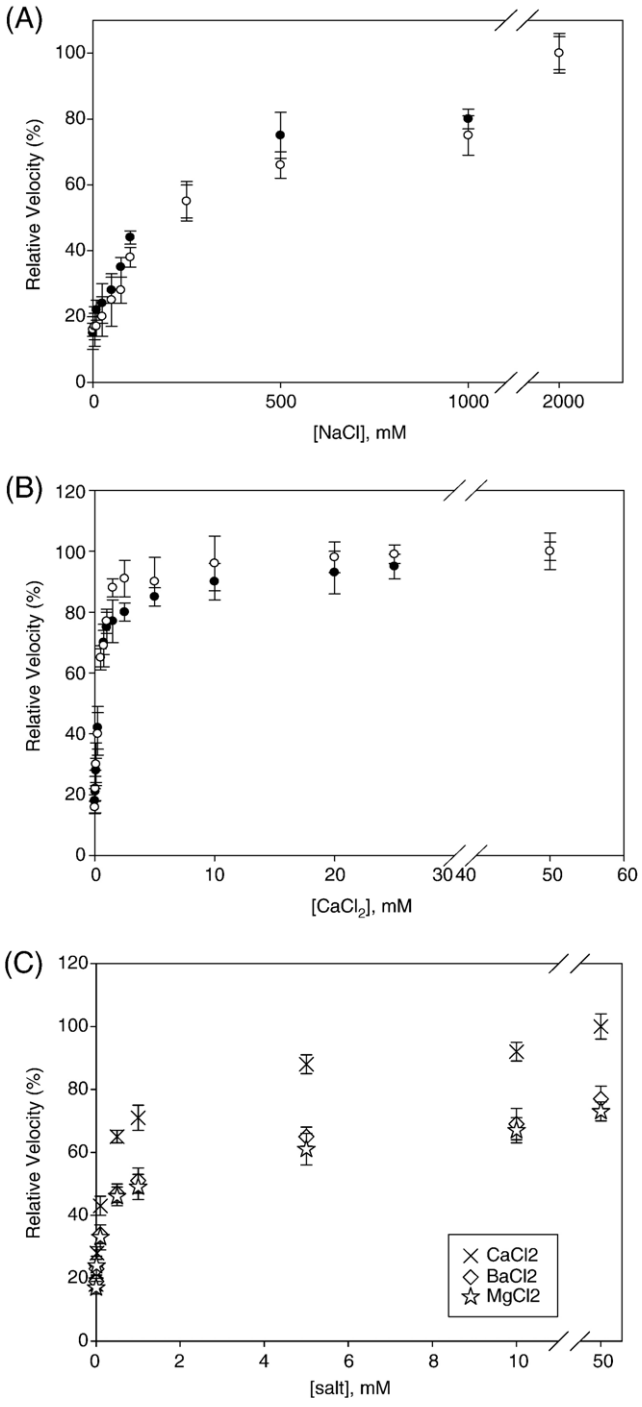

Fig. 6. Salt effects on 10 μg mL^{-1} crude venom metallopeptidase (○) and 0.1 mg mL^{-1} Bothropasin (●) activities over Abz-GGFLTSE-Q-EDDnp (10 μM), in 50 mM Tris–HCl, pH 7.4 at 37 °C. (A) NaCl effect, (B) $CaCl_2$ effect and (C) other divalent ions (Mg^{2+} and Ba^{2+}) in comparison to Ca^{2+}. Proportional rate of hydrolysis is shown as a function of the highest rate for each activity.

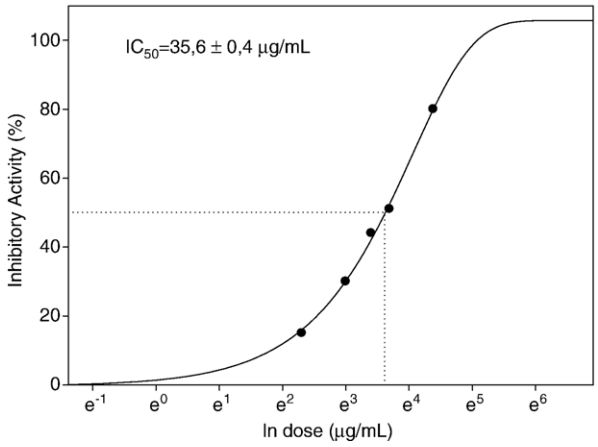

Fig. 7. Inhibition of the venom metallopeptidase activity. Monolog dose-dependency inhibition plot of the whole venom metallopeptidase (10 μg mL^{-1}) activity over Abz-GGFLTSE-Q-EDDnp (10 μM), in 50 mM Tris–HCl, pH 7.4, at 37 °C due to the addition of different doses of purified <EKW. Calculated IC_{50} is presented, corresponding to ~80 μM.

3.2. Enzymatic profiling of the venom

3.2.1. Activity pH dependence

The metallopeptidase activity of the venom of *B. jararaca* was assessed through the use of a specific FRET substrate, Abz-GGFLTSE-Q-EDDnp, originally designed as a target to SVMPs. The selectivity of the substrate for the venom metallopeptidases was confirmed by the use of 1 mM EDTA, which completely abolished the synthetic substrate hydrolysis, whilst 1 mM PMSF had no effect over the hydrolysis (data not shown). The peptide was cleaved by both the venom and bothropasin at the F–L bond as verified by HPLC (Fig. 4) and mass spectrometry analyses (not shown). The pH profiles presented in Fig. 5 show one peak of activity at pH 7.2 and are virtually identical for the isolated bothropasin and for the crude venom. There is no enzymatic activity below pH 4.5 and very little above pH 9. At pH 5.0, the native condition of the venom (Bonfim et al., 2006), activity remains less than 10% of the maximum. The calculated pK_a values for the crude venom metallopeptidase activity and for purified Bothropasin are virtually identical: 6.35±0.10 and 7.28±0.10 (venom) and 6.35±0.12 and 7.37±0.11 (Bothropasin).

3.2.2. Enzymatic activation through dilution

We also compared the venom metallopeptidase activity in its native concentrated form to the activity of the diluted venom. A series of diluted venom samples (1, 10, 16, 50, 75, 100, 1000 and 10,000-fold in 50 mM Tris–HCl, pH 7.4, containing 1 mM $CaCl_2$) were incubated with the substrate solution and hydrolysis was monitored by fluorescence monitoring by RP-HPLC. When the crude fresh venom was incubated with the FRET substrate,

little hydrolysis was detected by HPLC analysis. Fig. 4 presents representative superimposed fluorescence detection profiles of the RP-HPLC separated FRET substrate incubations with the crude venom and three representative serial dilutions. Under these conditions, a peak of activity, indicated by the highest substrate peak consumption, was found at a 100-fold dilution. Above this ratio, enzymatic activity started to decrease. Moreover, the fluorescent monitoring of the assays clearly indicates a single cleavage at the expected site.

3.2.3. Enzymatic modulation

3.2.3.1. Salt effect. We then analyzed the effect of salt concentration on the venom metallopeptidase and Bothropasin activities. The enzymatic activity of both the crude venom and Bothropasin were assessed in the presence of increasing concentrations of NaCl. Both the venom metallopeptidase and Bothropasin activities burst between 2 mM to 200 mM and then steadily rise up to 2 M NaCl (Fig. 6A).

3.2.3.2. Calcium modulation. The enzymatic activity of both the crude venom and Bothropasin were assessed in the presence of increasing concentrations of $CaCl_2$. For this assay, one can observe an exponential enzymatic activation in function of the addition of the salt. Again, this phenomenon was virtually identical for both the venom and Bothropasin activities (Fig. 6B). Furthermore, other divalent cations were assessed (Ba^{2+} and Mg^{2+}) and still Ca^{2+} demonstrated to be more effective on the specific enzymatic activation (Fig. 6C).

3.3. Peptidic inhibitor identification and characterization

Once a parallel between the Bothropasin activity and the crude venom metallopeptidase activity could be clearly established, including the pH dependency and salt effect, the identification of the main endogenous peptidic peptidase inhibitor in the venom could be performed.

All pooled fractions were tested for inhibition of the crude venom metallopeptidase activity (dashed bars, Fig. 1). Only the 4 final pools were able to differently inhibit the FRET substrate hydrolysis by the crude venom. Moreover, pool 113–119 was the most active fraction and was submitted to further chromatographic separations and biochemical characterizations (Figs. 2 and 3). The purified active peptide was de novo sequenced by ESI-Q-TOF-MS/MS mass spectrometry and has had its molar concentration determined by quantitative amino acid analysis and was demonstrated to be the tripeptide <EKW (being <E, pyroglutamic acid).

The purified peptide has had its inhibitory activity assessed over the venom metallopeptidase activity and has been shown to be able to inhibit it in a dose-dependant manner (Fig. 7). The IC_{50} value could be estimated from the monolog plot as being 35.6 μg mL^{-1} (~80 μM). Moreover, 1 mM $CaCl_2$ increases the IC_{50} of purified <EKW twice for the crude venom and five times for purified bothropasin (data not shown), when these metallopeptidase activities are assayed over the hydrolysis of the FRET substrate by 10 μg mL^{-1} crude *B. jararaca* venom or 0.1 mg mL^{-1} bothropasin in 50 mM Tris–HCl, pH 7.4 at 37 °C.

4. Discussion

One of the remarkable properties of the animal venoms is to kill or immobilize the prey in only few seconds. On the other hand, toxins, and particularly proteolytic enzymes, have to switch from an 'inactive' state inside the venom gland to a highly active form in the prey, in the same few seconds in order to perform their toxinic role. Therefore, fine-tuned mechanisms must exist in order to provide such regulations.

Bothrops venoms are, and have been for decades, largely studied both clinically and biochemically (Fox et al., 2006). Composition variations between species and even between genders within a given species are described (Furtado et al., 2006; Menezes et al., 2006) and novelties can still be found in this venom (Ianzer et al., 2004; Ponce-Soto et al., 2007; Bonfim et al., 2006). Interestingly, all these pieces of information do not sum up to form a clear and unequivocal picture in which the venom, its components, and the venom gland all fall into a straight toxic (or toxinic) pathway. For example, one can inquire from where all the 22 known BPPs (Ianzer et al., 2004; Pimenta et al., 2007) come, since only one proteic precursor (Murayama et al., 1997) has been found so far (at the nucleic acid level, not even as a protein) that contains only seven BPP sequences.

In this work, we demonstrated that there is a self proteolytic-regulation of the *B. jararaca* venom. Moreover, this regulation is based on a weak peptidic inhibitor ($IC_{50} \approx 80$ μM), whose potency of inhibition is strengthened by two physicochemical factors: namely, the acidic pH of the crude venom and the unavailability of ionic activators (due to chelation by citrate). Furthermore, we compared the whole crude venom metallopeptidase activity to the activity of the purified Bothropasin to ensure our findings.

Several authors have wandered around this subject and have been able to identify the few pieces of information that compose the whole inhibitory mechanism. However, as far as these authors' knowledge extend, none of them were able to perceive that it is not one separated feature, or even a paired association of features, as commented in (Fox et al., 2002), that is sufficient to cause a significant catalytic inhibition of the whole metallopeptidase activity of the *Bothrops* crude venom metallopeptidase activity (not its isolated enzymes, or a venom solution, as previously assessed by others).

We found that pH of the crude venom is the very first self-defense mechanism in the venom gland. Snake venom metallopeptidases are known to be most active between neutral and slightly alkaline conditions (Gomis-Ruth et al., 1994). Our results show that the metallopeptidase activity of the whole *B. jararaca* venom and Bothropasin is higher at pH 7.2, while it is still fairly low at pH 5.0 (Fig. 5), which is the native condition of the venom (Cidade et al., 2006). From this we can say that pH alone is one important inhibitory factor of the venom metallopeptidase activity inside the snake's venom gland. This is in accordance to the well established fact that the protonation of aspartate and glutamate carboxylates in the calcium binding sites impair hydrolysis.

Second, ionic composition (or availability) plays an important role in restraining the metallopeptidase activity. Several

authors have suggested that citrate is responsible for the inactivity of SVMPs against the venom own constituents inside the venom gland. Citrate is a divalent cation chelator and is present in *Bothrops* snakes at concentrations between 58 and 125 mM (Odell et al., 1998), which should be enough to remove all free calcium and zinc present in the venom. Calcium has been shown to reside on the surface of the SVMPs, opposite to the catalytic site (Gossas and Danielson, 2006), but the crystallographic studies of SVMP do not show how the calcium ion detected in these structures could be related to catalysis. Our experiments clearly indicate two very distinct roles for the assayed cations: Na^+ followed a clear kosmotropic salt activation profile (Fig. 6A), clearly belonging to the Hofmeister series (Baldwin, 1996), in which enzymatic activation is due to a salting-in effect that causes protein stabilization rather than specific activation (Gomis-Ruth et al., 1994). Ca^{2+}, on the other hand, presented an exponential activation profile (Fig. 6B), which was specific to this divalent cation (Fig. 6C). This kind of curve suggests the saturation of one or more calcium binding sites on the enzymes, in agreement with structural data from several P-I SVMPs in which a calcium ion is located on the surface of the enzyme opposite to the catalytic site (Gomis-Ruth et al., 1994; Zhang et al., 1994; Zhu et al., 1999). Bothropasin is a P-III SVMP and it is possible that other calcium binding sites exist in the disintegrin and cysteine-rich domains. Recently, Takeda et al. (2006) have published the resolved tridimensional structure of vascular apoptosis-inducing protein-1 (VAP1), a disulfide-bridged homodimer P-III SVMP isolated from *Crotalus atrox* venom and revealed the details of the stabilizing calcium ions bound to the molecule.

The third is the presence of a peptidic peptidase inhibitor. Other authors consider the venom pyroglutamyl tripeptides as at least partly responsible for the inhibition of SVMPs in the gland (Robeva et al., 1991; Gomis-Ruth et al., 1998). While it is true that they can inhibit these enzymes, at least partially, they certainly are not the only inhibiting factor involved, as the two factors presented above are definitely important. Peptide inhibitors of metallopeptidases basically act by competing with the substrates, binding to the zinc ion in the catalytic site, preventing hydrolysis. This mechanism should be very dependant on the enzyme conformation, since <EKW significantly looses its ability to inhibit the crude venom metallopeptidase activity or bothropasin in the presence of 1 mM $CaCl_2$.

Moreover, not a single bradykinin potentiating peptide (BPP), which comprises an undoubtfully efficient metallopeptidase inhibitor class for enzymes *other* than those isolated from the venom, has been identified so far as an astonishing SMVP inhibitor. Even with our own work, which has inflated the *Bothrops* BPP pool in ~60% over the past years (Ianzer et al., 2004; Pimenta et al., 2007), no specific SVMP BPP has been found. Based on these previous publications of ours and accumulated knowledge on the *B. jararaca* venom, we can assure that fraction 113–119 contains several BPPs (Fig. 2A, m/z=612.3; 654.3; 1101.6; 1196.6 and 1299.7 just to mention a few) that were not selected throughout the biological driven assay employed in this work as the physiological SVMP inhibitor.

On the other hand, that is highly desirable in an enzymatic sense. If the snake inhibited its own enzymes with a very efficient (low k_{-1} value) and/or tight-binding inhibitor (very low k_1 and low k_{-1} values), than the inhibitor release from the enzyme active site would be much more difficult and slow, and rely on larger dilution volumes and/or longer times, which would be incompatible with their typical prey size and/or available time-frame for capturing the prey or fleeing. In other words, the venom would not work.

Whether calcium interacts directly with the inhibitor, preventing its interaction with the enzyme is purely speculative, but from our results, we would suggest that citrate plays a double role in the inhibition: first, by preventing the activation of the SVMPs by calcium (due to chelation, which can be speculated even to involve the catalytic Zn as well as a function of the high citrate concentration present) and, second, by potentiating the inhibition of SVMPs by the pyroglutamyl tripeptide. Given the highly aggressive nature of the SVMPs, a redundant mechanism of inhibition is not surprising in order to protect the gland tissues and venom components from their action. The mechanism of prevention of the inhibition by the peptide inhibitors in the presence of calcium remains to be determined.

Taken together, all these three rather simple and weak (on their own) inhibitory mechanisms sum up to a very solid and redundant self-proteolysis regulation system. The experiment showing an increase in the metallopeptidase activity, over a FRET substrate, when the venom is diluted up to 100-fold, decreasing only thereafter, was planned to resemble the envenomation process (Fig. 4). Upon inoculation, the crude venom faces instant dilution into the prey's blood stream. Citrate concentration drops immediately so that no Ca^{2+} (or Zn^{2+}) chelation can occur anymore. Moreover, <EKW weak peptidic inhibitors (IC_{50} ~ 80 μM, totally in accordance to (Huang et al., 1998), who have estimated this value as being ~250 μM for *T. mucrosquamatus*) also unbinds from the enzyme active site, once there is no more highly concentrated microenvironment that would guarantee peptidase inhibition at such a poor K_i value. There was little hydrolysis observed at the 'crude' venom aliquot, though. We hypothesize that this hydrolysis is ought to be due to some minute dilution of the crude venom in to the substrate solution or some unspecific serinopeptidase; but, there was a clear pattern of enzymatic activation through dilution up to 100-fold, and subsequent decrease.

Venom stability has been assessed by authors studying not only *B. jararaca* venom, but toxins from the most diverse species. Sousa's work on the proteic stability of *B. jararaca* venom deals with specific effects such as coagulant activity, hemagglutinating activity and azocaseinolytic activity and the alteration pattern of the SDS-PAGE of the crude venom over time and under different dilution conditions. Authors state that "in the conditions used in (their) study, venom solutions (0.5 mg/mL) are at least 125-fold less concentrated than fresh venom and obviously citrate and other possible endogenous protease inhibitors are less concentrated than in vivo. Other mechanisms that regulate metal-independent serine proteases from venom may also exist to prevent their action on other constituents during venom formation". In this sense, the present work adds a few pieces of information in order

to clarify the mechanisms of venom and tissue preservation within the gland.

Marino et al. (2007) have studied toxicity and stability properties of crude venom from isolated nematocysts of *Pelagia noctiluca* (Cnidaria, Scyphozoa) and, by monitoring its hemolytic activity, have demonstrated that the toxins present in the venom retain their toxicity under the harshest conditions, such as wide pH variation, high temperatures and protease incubation, even though authors point out the possible proteic and peptidic nature of the toxins. However, Marino's work does not address the mechanisms of inhibition of the crude venom and protection of the gland tissues (or nematocyst's structure) in the way we analyze the bothropic venom and its inhibition within the venom gland. Winter et al. (2007) have explored the crude venom of an Australian jellyfish (*Chironex fleckeri*) in a very similar way to Marino's, *e.g.*, pH and temperature variations and stability upon lyophilization, but also not in regard to the nematocyst and its integrity.

Monroy-Estrada et al. (2007), Samy et al. (2007), Porto et al. (2007) and Sivan et al. (2007) have dealt with crude venoms from different sources and their biological activities on several systems. However, these authors do not asses the storage conditions and possible activation mechanisms of these venoms. Those works focus on the biological and toxic effects of the venoms and their constituents, regardless of their origin.

Xu et al. (2007) study metal ions- and pH-induced conformational changes of acutolysin A from *Agkistrodon acutus*. Authors report the protective effect of Ca^{+2} and Zn^{+2} over the pH-induced denaturation of this metallopeptidase and the effects on the proteolytic activity. Parallels can be made with the current study and the protective effect of citrate on the integrity of the *B. jararaca* venom gland.

Perhaps the most direct comparison of our study should be made with the work of Munekyio and Mackessy (2005) which have investigated the distribution of <EQW and <ENW in venoms from nine species of rattlesnakes and evaluated the role of these peptides in inhibiting and stabilizing isolated major venom metalloproteases (Cvo Pr V and cromipyrrhin) from *Crotalus oreganus oreganus* and *C. mitchelli pyrrhus* venoms. Although authors initially focus on the long-term storage of proteins aiming to preserve their biological activity for potential protein-drugs design, they recur to the fact that a model for the long-standing stabilization of proteins already exists in natural systems, particularly among viperid snakes. These animals' venoms are rich in lytic enzymes that are secreted into the lumen of the gland and can be stored in an inactive, yet competent, state for many months. For these authors, one mechanism capable of inhibiting autolysis is the production of (relatively) low affinity peptide enzyme inhibitors. Moreover, authors even raise the same point we present here, that is that together with other mechanisms which inhibit venom enzymes (low pH, high citrate levels, cysteine switch activation), the peptide inhibitors stabilize and inhibit autolytic proteins, thereby protecting venom integrity during long-term storage and protecting the snake against potential damage by its own venom components.

In summary, by evolving in this sense, *e.g.*, choosing the combination of three relatively weak and independent inhibitory pathways, the *B. jararaca* venom (and its constituents) has come to a perfect balance between self-molecular and tissular integrity safeguarding and rapid and efficient physiopathological effect upon prey biting.

Acknowledgement

This study is supported by FAPESP (including post-doctoral grant # 01/01018-6). We also acknowledge Dr K. Konno for technical assistance and Dr A. M. Moura-da-Silva for Bothropasin aliquots. We are grateful to Dr A.C.M. Camargo for the use of the CAT/CEPID facilities.

References

Assakura, MT, Silva, CA, Mentele, R, Camargo, AC, Serrano, SM, 2003. Molecular cloning and expression of structural domains of bothropasin, a P-III metalloproteinase from the venom of *Bothrops jararaca*. Toxicon 41, 217–227.

Baldwin, RL, 1996. How hofmeister ion interactions affect protein stability. Biophys. J. 71, 2056–2063.

Blundell, TL, 1994. Metalloproteinase superfamilies and drug design. Nat. Struct. Biol. 1, 73–75.

Bonfim, VL, Ponce-Soto, LA, Novello, JC, Marangoni, S, 2006. Cytotoxic action in myoblasts and myotubes (C2C12) and enzymatic characterization of a new phospholipase A2 isoform (Bj-V) from *Bothrops jararacussu* venom. Protein Pept. Lett. 13, 707–713.

Cidade, DA, Simao, TA, Davila, AM, Wagner, G, Junqueira-de-Azevedo, IL, Ho, PL, Bon, C, Zingali, RB, Albano, RM, 2006. *Bothrops jararaca* venom gland transcriptome: analysis of the gene expression pattern. Toxicon 48, 437–461.

Fox, JW, Serrano, SMT, 2005. Structural considerations of the snake venom metalloproteinases, key members of the M12 reprolysin family of metalloproteinases. Toxicon 45, 969–985.

Fox, JW, Ma, L, Nelson, K, Sherman, NE, Serrano, SM, 2006. Comparison of indirect and direct approaches using ion-trap and Fourier transform ion cyclotron resonance mass spectrometry for exploring viperid venom proteomes. Toxicon 47, 700–714.

Fox, JW, Shannon, JD, Stefansson, B, Kamiguti, AS, Theakston, RDG, Serrano SMT Camargo, ACM, Sherman, N, 2002. Role of discovery science in toxinology: examples in venom proteomics. In: Menez, A. (Ed.), Perspectives in Molecular Toxinology. Wiley, UK, pp. 97–108.

Furtado, MF, Travaglia-Cardoso, SR, Rocha, MM, 2006. Sexual dimorphism in venom of *Bothrops jararaca* (Serpentes: Viperidae). Toxicon 48, 401–410.

Gomis-Ruth, FX, Grams, F, Yiallouros, I, Nar, H, Kusthardt, U, Zwilling, R, Bode, W, Stocker, W, 1994. Crystal structures, spectroscopic features, and catalytic properties of cobalt(II), copper(II), nickel(II), and mercury(II) derivatives of the zinc endopeptidase astacin. A correlation of structure and proteolytic activity. J. Biol. Chem. 269, 17111–17117.

Gomis-Ruth, FX, Meyer, EF, Kress, LF, Politi, V, 1998. Structures of adamalysin II with peptidic inhibitors. Implications for the design of tumor necrosis factor alpha convertase inhibitors. Protein Sci. 7, 283–292.

Gossas, T, Danielson, UH, 2006. Characterization of Ca2+ interactions with matrix metallopeptidase-12: implications for matrix metallopeptidase regulation. Biochem. J. 398, 393–398.

Huang, KF, Hung, CC, Wu, SH, Chiou, SH, 1998. Characterization of three endogenous peptide inhibitors for multiple metallopeptidases with fibrinogenolytic activity from the venom of Taiwan habu (*Trimeresurus mucrosquamatus*). Biochem. Biophys. Res. Commun. 248, 562–568.

Ianzer, D, Konno, K, Marques-Porto, R, Vieira Portaro, FC, Stocklin, R, Camargo, ACM, Pimenta, DC, 2004. Identification of five new bradykinin potentiating peptides (BPPs) from *Bothrops jararaca* crude venom by using electrospray ionization tandem mass spectrometry after a two-step liquid chromatography. Peptides 25, 1085–1092.

Jia, LG, Wang, XM, Shannon, JD, Bjarnason, JB, Fox, JW, 1997. Function of disintegrin-like/cysteine-rich domains of atrolysin A. Inhibition of platelet

aggregation by recombinant protein and peptide antagonists. J. Biol. Chem. 272, 13094–13102.

Mandelbaum, FR, Reichel, AP, Assakura, MT, 1982. Isolation and characterization of a proteolytic enzyme from the venom of the snake *Bothrops jararaca* (Jararaca). Toxicon 20, 955–972.

Marino, A, Crupi, R, Rizzo, G, Morabito, R, Musci, G, La Spada, G, 2007. The unusual toxicity and stability properties of crude venom from isolated nematocysts of *Pelagia noctiluca* (Cnidaria, Scyphozoa). Cell Mol. Biol. (Noisy-le-grand) 53 (Suppl:OL), 994–1002.

Menezes, MC, Furtado, MF, Travaglia-Cardoso, SR, Camargo, AC, Serrano, SM, 2006. Sex-based individual variation of snake venom proteome among eighteen *Bothrops jararaca* siblings. Toxicon 47, 304–312.

Monroy-Estrada, HI, Segura-Puertas, L, Galván-Arzate, S, Santamaría, A, Sánchez-Rodríguez, J, 2007. The crude venom from the sea anemone *Stichodactyla helianthus* induces haemolysis and slight peroxidative damage in rat and human erythrocytes. Toxicol. In Vitro 21, 398–402.

Moura-da-Silva, AM, Della-Casa, MS, David, AS, Assakura, MT, Butera, D, Lebrun, I, Shannon, JD, Serrano, SM, Fox, JW, 2003. Evidence for heterogeneous forms of the snake venom metallopeptidase jararhagin: a factor contributing to snake venom variability. Arch. Biochem. Biophys. 409, 395–401.

Munekiyo, SM, Mackessy, SP, 2005. Presence of peptide inhibitors in rattlesnake venoms and their effects on endogenous metalloproteases. Toxicon 45, 255–263.

Murayama, N, Hayashi, MA, Ohi, H, Ferreira, LA, Hermann, VV, Saito, H, Fujita, Y, Higuchi, S, Fernandes, BL, Yamane, T, Camargo, AC, 1997. Cloning and sequence analysis of a *Bothrops jararaca* cDNA encoding a precursor of seven bradykinin-potentiating peptides and a C-type natriuretic peptide. Proc. Natl. Acad. Sci. U. S. A. 94, 1189–1193.

Odell, GV, Ferry, PC, Vick, LM, Fenton, AW, Decker, LS, Cowell, RL, Ownby, CL, Gutierrez, JM, 1998. Citrate inhibition of snake venom proteases. Toxicon 36, 1801–1806.

Pimenta, DC, Prezoto, BC, Konno, K, Melo, RL, Furtado, MF, Camargo, AC, Serrano, SM, 2007. Mass spectrometric analysis of the individual variability of *Bothrops jararaca* venom peptide fraction. Evidence for sex-based variation among the bradykinin-potentiating peptides. Rapid Commun. Mass Spectrom. 21, 1034–1042.

Ponce-Soto, LA, Lomonte, B, Gutierrez, JM, Rodrigues-Simioni, L, Novello, JC, Marangoni, S, 2007. Structural and functional properties of BaTX, a new Lys49 phospholipase A(2) homologue isolated from the venom of the snake *Bothrops alternatus*. Biochim. Biophys. Acta 1770, 585–593.

Porto, BN, Telli, CA, Dutra, TP, Alves, LS, Bozza, MT, Fin, CA, Thiesen, FV, Renner, MF, 2007. Biochemical and biological characterization of the venoms of *Bothriopsis bilineata* and *Bothriopsis taeniata* (Serpentes: Viperidae). Toxicon 50, 270–277.

Robeva, A, Politi, V, Shannon, JD, Bjarnason, JB, Fox, JW, 1991. Synthetic and endogenous inhibitors of snake venom metalloproteinases. Biomed. Biochim. Acta 50, 769–773.

Samy, RP, Gopalakrishnakone, P, Thwin, MM, Chow, TK, Bow, H, Yap, EH, Thong, TW, 2007. Antibacterial activity of snake, scorpion and bee venoms: a comparison with purified venom phospholipase A2 enzymes. J. Appl. Microbiol. 102, 650–659.

Sivan, G, Venketesvaran, K, Radhakrishnan, CK, 2007. Biological and biochemical properties of *Scatophagus argus* venom. Toxicon 50, 563–571.

Sousa, JR, Monteiro, RQ, Castro, HC, Zingali, RB, 2001. Proteolytic action of *Bothrops jararaca* venom upon its own constituents. Toxicon 39, 787–792.

Takeda, S, Igarashi, T, Mori, H, Araki, S, 2006. Crystal structures of VAP1 reveal ADAMs' MDC domain architecture and its unique C-shaped scaffold. EMBO J. 25, 2388–2396.

Winter, KL, Isbister, GK, Seymour, JE, Hodgson, WC, 2007. An in vivo examination of the stability of venom from the Australian box jellyfish *Chironex fleckeri*. Toxicon 49, 804–809.

Xu, X, Chen, J, Zhang, L, Liu, Q, 2007. Metal ions- and pH-induced conformational changes of acutolysin A from *Agkistrodon acutus* venom probed by fluorescent spectroscopy. Biopolymers 85, 81–90.

Zhang, D, Botos, I, Gomis-Ruth, FX, Doll, R, Blood, C, Njoroge, FG, Fox, JW, Bode, W, Meyer, EF, 1994. Structural interaction of natural and synthetic inhibitors with the venom metalloproteinase, atrolysin C (form d). Proc. Natl. Acad. Sci. U. S. A. 91, 8447–8451.

Zhu, X, Teng, M, Niu, L, 1999. Structure of acutolysin-C, a haemorrhagic toxin from the venom of *Agkistrodon acutus*, providing further evidence for the mechanism of the pH-dependent proteolytic reaction of zinc metalloproteinases. Acta Crystallogr., D Biol. Crystallogr. 55, 1834–1841.